DTC of Open End Winding Induction Motor fed by cascaded Space Vector modulated inverters

G.Satheesh, T. Bramhananda Reddy
Department of EEE
G.P.R.E.C., Kurnool, Andhra Pradesh., India
gsatish.eee@gmail.com; tbnr@rediffmail.com

CH. Sai Babu
Department of Electrical Engineering,
J. N. T. U., Kakinada, Andhra Pradesh., India
chs.eee@gmail.com

Abstract—**This paper proposes two control strategies, Decoupled and Nearest Sub Hexagon Center (NSHC) algorithms for the open-end winding configuration of induction motor. A space vector pulse width modulation (SVPWM) based 3-level voltages are generated in both methods with two 2-level inverters. In these two methods, inverter-1 pulses are generated normally and inverter-2 pulses are generated with 180^o phase shift, resulting a 3-level line voltage waveform to the induction motor. In the first method inverter-1 output is superimpose on inverter-2 output with the both inverters are switching at the same frequency in all states. In the second method at a particular state of switching inverter-1 is switched in all states and inverter-2 is clamped to one active state, vice versa in the next state of switching. It uses the concept of imaginary switching times for SVPWM with direct torque control (DTC). The imaginary switching times greatly simplifies the algorithms. This method also eliminates the procedure for identifying the region for space voltage vector. Also, it does not require the sectors and angle identification of the voltage vector. Simulation studies have been carried out for the proposed scheme. Results have been presented to validate the proposed schemes.**

Keywords- Decoupled Algorithm, DTC, Dual Inverter, NSHC Algorithm, OEWIM, svpwm.

I. INTRODUCTION

The main aim of the multi level inverters is to produce a high voltage output using the devices with standard voltages. One such a technique is cascading of two 2-level inverters. With this concept the same maximal 3-level voltage output can be achieved [1] as in the conventional 3-level inverter. The induction motors which are using for the low and medium power level applications are later changed to the high power level applications by feeding the 3 phase stator winding with two separate 2-level inverters. The direct torque control (DTC) for the high power induction motors was proposed [2] two decades back. Numerous of researches have been carried out on the DTC of the induction motor in the past years and proposed number of control techniques for the Open End Winding Induction Motor drive. The work presented in [3] is results in Torque and speed fluctuations, higher ripple in the stator current. Direct Self Control technique has been proposed for machine with open-end winding configuration with two 3 level inverters at both ends [4]. But with the three level inverters on both ends leads to increment in cost and complexity. The open-end winding configuration has been proposed for high power electric vehicle/ hybrid electric vehicle (EV/HEV) propulsions systems [5]. In [1] a Space Vector Pulse Width Modulation (SVPWM) technique is used to control the output voltage of two inverters connected at both ends of the motor winding. It should be noted that the switching frequency capacity of both the inverters is same. In

[1] and [6] the schemes proposed are complex due to identification of the region since the entire region is divided in 24 small regions or in to 7 small regions. In order to reduce the complexity of the sector/region identification a SVPWM method for open-end winding configuration has been proposed using the concept of imaginary switching times [7]. It does not require any sector or sub-sector identification. It greatly simplifies the control strategy. Also, the switching frequency of both the inverters is same. But the above schemes are having more harmonics in voltage profile.

In this paper, the Decoupled, Nearest Sub Hexagon Center (NSHC) switching schemes are proposed, the results and harmonics in voltage and current profiles are discussed.

II. OPEN – END WINDING INDUCTION MOTOR

A schematic of the open-end winding induction motor drive is shown in Figure. 1. Two 2-level inverters, INV-I, feeds the three ends of the stator winding A, B, C and the INV-2 feeds the three ends A', B' and C'. INV-1and INV-2 are connected to two separate dc sources with magnitude of Vdc/2 to avoid the zero sequence currents.

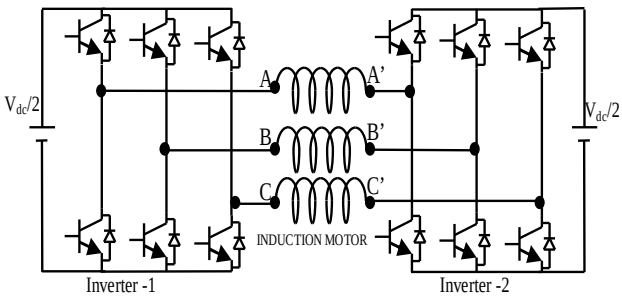

Figure 1. Open-End winding configuration of the Induction Motor Drive

Figure. 2 and Figure. 3 presents the switching state vectors of two individual inverters and 3 level space vector combination. The conventional definition for the switching state sequence of the switches for the phases of ***ABC*** of each individual inverter is used here. In particular, for INV-1: **1** – 100; **2** – 110; **3** – 010; **4** –011; **5** – 001; **6** – 101. 1 - switch-on state, 0 – switch-off state; and the same definition are used for INV-2: **1'** – 1'0'0'; **2'** – 1'1'0'; **3'** – 0'1'0'; **4'** – 0'1'1'; **5'** – 0'0'1'; **6'** – 1'0'1', where 1' - switch-on state of switches of INV2, and 0' – switch-off state in INV-2. The pole voltages of INV-1 are V_{a0}, V_{b0}, V_{c0} and, the pole voltages of INV-2 are $V_{a'0}$, $V_{b'0}$, $V_{c'0}$. Any leg of the two inverters can independently

attain levels 0 or Vdc/2. The voltage across a particular phase winding can be obtained

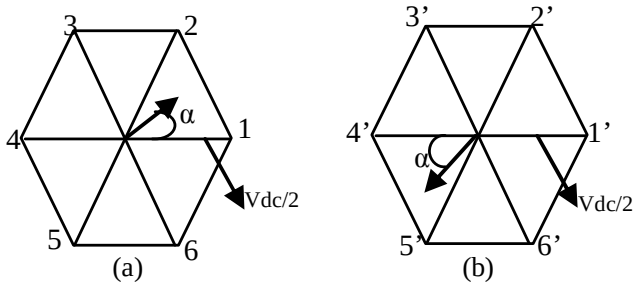

Figure 2. Switching state vectors of two individual Inverters (a) Inverter-1, (b) Inverter-2

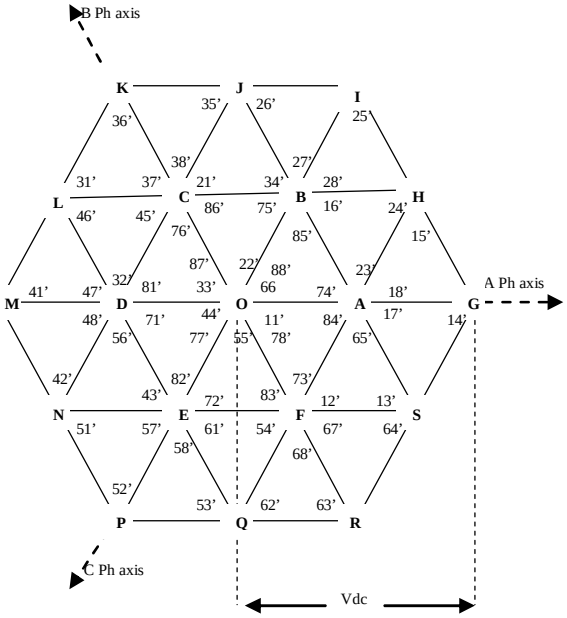

Figure 3. Three-level Voltage Space Vectors locations

by

$$V_{aa'} = V_{a0} - V_{a'0} \quad (1)$$

$$V_{bb'} = V_{b0} - V_{b'0} \quad (2)$$

$$V_{cc'} = V_{c0} - V_{c'0} \quad (3)$$

The effective phase voltages in the three windings can be represented by a voltage space vector as defined by

$$V_{ref} = V_{aa'} + V_{bb'} e^{j2\pi/3} + V_{cc'} e^{j4\pi/3} \quad (4)$$

This voltage space vector can be equivalently represented as the sum of the voltage space vectors generated by the two 2-level inverters in the Figure. 5. The 3 level output of the effective space phasor voltage is represented in the Figure. 3 contains 64 vector location with 24 sectors Figure. 3 and Figure. 5. Six adjacent sectors together form a hexagon. Six such hexagons can be identified with their centers located at A, B, C, D, E, and F respectively. In addition there is one inner hexagon with its center at 0. Based on these sub-hexagons, a space phasor based PWM scheme is proposed in the same way as in the case of the conventional three phase inverter [8].

The switching algorithm described in reference [10] for a 2-level inverter feeding a conventional induction motor is extended for the dual-inverter system to compute the switching timings for individual inverters.

III. PROPOSED PWM STRATEGIES

The specified algorithm in [10] uses only the instantaneous reference voltages and is based on the concept of 'effective time'. The effective time is defined as the time "when the inverter supplies power to the motor in a given sampling time period and is denoted as T_{eff}. The sampling time period is denoted as T_s. The instantaneous phase reference voltages are obtained by projecting the tip of the reference vector Vsr on to the respective phase axes and multiplying the values of these projections with a factor of (2/3). The factor (2/3) arises because of the classical 'Two to Three phase' transformation. These instantaneous phase reference voltages are denoted as V_a*, V_b* and V_c*. The symbols Tga, Tgb and Tgc respectively denote the time duration for which a given motor phase is connected to the positive rail of the input DC power supply of the inverter in the given sampling time period Ts. The timings Tga, Tgb and Tgc are termed as the phase switching times. The procedure to generate the gating pulses for the individual devices using this algorithm is elaborately explained in [10]. For a dual inverter system, there would be two sets of phase switching times, one for each inverter. The phase switching timings of inverter-1 are denoted by the symbols Tga, Tgb and Tgc , while the symbols T'ga, T'gb and T'gc denote the same for inverter-2.

With the above effective concept here are the proposed PWM strategies a) The Decoupled PWM strategy b) The Alternative Inverter switching strategy

Few observations are made for the above strategies they are a) To obtain the 3 level output first inverter output is superposed on the second inverter output at each vector location. b) Hexagon ABCDEF with center O is named as core

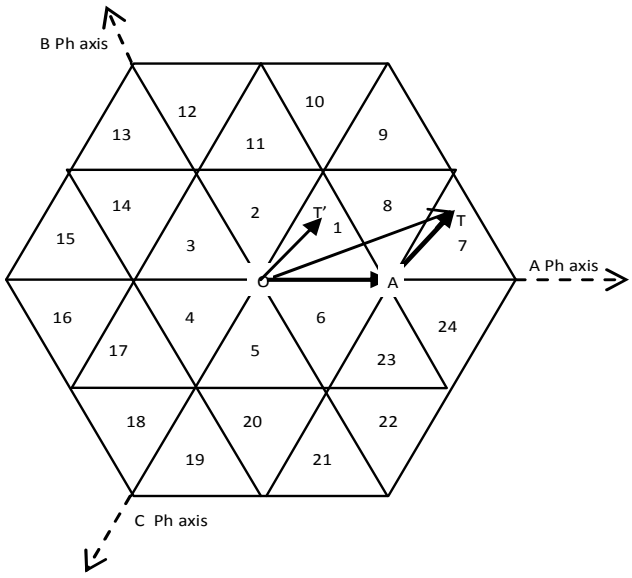

Figure 4. Reference space vector for 3 level voltages

hexagon, there exist six outer hexagons namely OBHGSF, OCJIHA, ODLKJB, OENMLC, OFQPND and OASRQE centered around the points A, B, C, D, E and F respectively these are referred to as sub-hexagonal centers. c)The space vector combinations at the vertices and at the center of a given sub- hexagon are obtained by clamping one inverter to a given state while the other inverter switches in all the eight states.

IV. DECOUPLED PWM STRATEGY

This PWM strategy is based on the fact that the reference voltage space vector V_{sr} can be constructed with two opposite components $V_{sr}/2$ and $-V_{sr}/2$. Subtraction of the second component from the first achieves the desired reconstruction of the reference vector. In other words, it is based on the observation that the effect of applying a vector with inverter-1 while inverter-2 assumes a null state is twice as that of applying the opposite vector with inverter-2 while inverter-1 assumes a null state. Figure. 2 and Figure. 4 show the method of this PWM strategy. It is worth noting that the phase axes of the motor viewed with reference to individual inverters are in phase opposition. In Figure. 2 and Figure. 3, the vector **OT** represents the actual reference voltage space vector, which is to be synthesized from the dual-inverter system and is given by |Vsr |∠αThis vector is resolved into two opposite components OT_1 is (|Vsr/2 |∠α) and $O'T_2$ is (|Vsr/2 | $\angle 180^0$ + α). The vector OT_1 is synthesized by inverter-1 in the average sense by switching amongst the states (8-1-2-7) while the vector $O'T_2$ is reconstructed by inverter-2 in the average sense by switching amongst the states (8'-5'-4'-7'). The switching algorithm described in reference [10] for the implementation of space vector modulation for a 2-level inverter feeding a normal induction motor is extended for the computation of the switching timings for individual inverters of the dual-inverter system. The advantage with the proposed decoupled control is that the inverter switching timings of both the inverters need not be computed. However, in this approach, both inverters are to be switched.

V. NSHC SWITCHING STRATEGY

This scheme is based on the observation of that the space vector combinations at the vertices and the center of a given sub hexagon are obtained by clamping one inverter with an active state, while the other inverter switches in all eight states. The center of the nearest sub hexagon is obtained from the instantaneous reference voltage quantities which will be discussed here in further steps.

In the figure – 4, Vector OT represents the reference vector with its tip located in sector 7 (in the triangle AHG). It is resolved in to two components OA and AT. The vector OA may be output of inverter -1which is clamped to state 1 (+ - -) through the sampling interval and the vector AT may be the output of other inverter -2, which is switched in all eight states. i.e the inverter -2 is switched with center A (the nearest sub hexagon center of OFSGHB). Otherwise the first vector OA is the output of the inverter -2 which is clamped to the state 1 (+ - -) and the vector AT is the generated by switching the inverter -1. At each step of the interval the nearest sub hexagon center is identified by resolving the OT vector in to two components and first component is the output of the one inverter by clamped to an active state and other inverter is switched in all eight centers. In this scheme for the odd numbered centers inverter -1 is clamped i.e for A, C, E sub hexagon centers and the inverter -2 is switched, and for the other centers i.e B, D, F center sub hexagons inverter -1 is clamped and inverter -2 is switched. The roles of the individual inverters at each center is summarises in Table. 1.

Table. 1. Roles of Individual inverters at each NSH centers

Center	*A*	*B*	*C*	*D*	*E*	*F*
Inverter -I	Switching	Clamped to B	Switching	Clamped to D	Switching	Clamped to F
Inverter -II	Clamped to A	Switching	Clamped to C	Switching	Clamped to E	Switching

The instantaneous phase reference voltage denoted by Vas, Vbs, Vcs corresponding to the reference voltage space vector OT are obtained by projecting the tip of OT onto the respective phase axes and multiplying them by a factor (2/3). The symbols Vds and Vqs denote the components of OT on the d and q axes, respectively. The reference voltages corresponding to the actual switching vector AT, denoted by Va, Vb and Vc, are obtained by the following procedure:

1. By using classical 3phase to 2 phase transformation method we can obtain the equivalent two-phase system references Vds and Vqs of the reference vector OT from the instantaneous phase reference voltages Vas, Vbs and Vcs.

$$\begin{bmatrix} Vds \\ Vqs \end{bmatrix} = \begin{bmatrix} \frac{3}{2} & 0 & 0 \\ 0 & \frac{\sqrt{3}}{2} & -\frac{\sqrt{3}}{2} \end{bmatrix} \begin{bmatrix} Vas \\ Vbs \\ Vcs \end{bmatrix}$$

2. The Sub Hexagonal Center situated nearest to the tip of the reference vector OT is then determined.

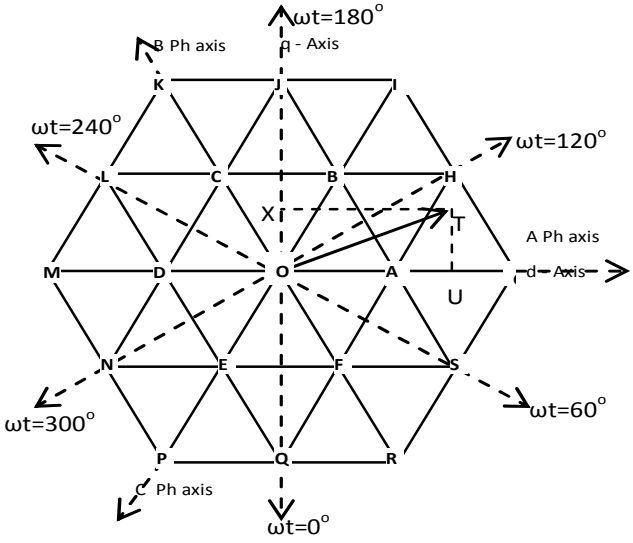

Figure. 5. Principle of Nearest Sub-Hexagon switching scheme

3. The coordinates of the nearest Sub Hexagonal Center (NSHC) in the Vd – Vq plane (the point 'A' in this example, Fig. 5), denoted by *Vdnshc* and *Vqnshc* are identified for all the six Sub Hexagonal Center s. For example, the coordinates of the point 'A' in the Vd – Vq plane are given by (Vdc/2, 0), similarly the coordinates of the point 'D' in the Vd –Vq plane are given by (-Vdc/2, 0).

4. Since the vector OA is output by the clamping inverter, the coordinates of the switching vector (AT in the present case) denoted by *Vdsw* and *Vqsw* are given by

$$Vdsw = \text{Vds} - Vdnshc$$

$$and \;\; Vqsw = \text{Vqs} - Vqnshc$$

5. By using the classical two-phase to three-phase transformation, the modified reference phase voltages Vasw, Vbsw and Vcsw for the switching inverter are then obtained by transforming *Vdsw*, *Vqsw* into the corresponding three-phase variables

$$\begin{bmatrix} Vasw \\ Vbsw \\ Vcsw \end{bmatrix} = \begin{bmatrix} \frac{2}{3} & 0 \\ -\frac{1}{3} & \frac{1}{\sqrt{3}} \\ -\frac{1}{3} & -\frac{1}{\sqrt{3}} \end{bmatrix} \begin{bmatrix} Vdsw \\ Vqsw \end{bmatrix}$$

6. If inverter-2 is employed as the clamping inverter, the modified references are used directly to generate the switching vector AT with inverter-1. On the other hand, if inverter-1 is used as the clamping inverter, it is obvious that the modified references must be negated to generate the switching vector AT with inverter-2.

7. It is important to note that the most important part of this algorithm is to find the nearest sub hexagonal center to the tip of the reference vector OT. The instantaneous reference voltages Vas, Vbs and Vcs normalised with respect to Vsr and their respective negations are shown in figure. 6.

From the figure.6, it may be noted that Vas is more positive quantity amongst these six quantities when $60^o \leq \theta \leq 120^o$ and A is the nearest sub hexagonal center as recognized by figure 5. Similarly –Vas is the most positive amongst these six quantities when $240^o \leq \theta \leq 300^o$ and D is the nearest sub hexagonal center. Thus it is clear that by finding the maximum value amongst these six quantities, one can determine the nearest sub hexagonal center.

The basic switching algorithm described in [10] for the classical case of a two-level inverter feeding the conventional three-phase induction motor is extended for the dual-inverter system to compute the switching timings for individual inverters. This algorithm accomplishes the automatic generation of the gating pulses for the individual switching devices while placing the effective time exactly at the centre of a given sampling time period. The effective time is defined as the time for which the inverter supplies power to the motor in a given sampling time period and is denoted by Teff . The sampling time period is denoted by Ts. The symbols Tga, Tgb and Tgc, respectively, denote the time duration for which a given motor phase is connected to the positive rail of the input DC power supply of the inverter in the given sampling time period Ts. The timings Tga, Tgb and Tgc are termed as the phase switching times.

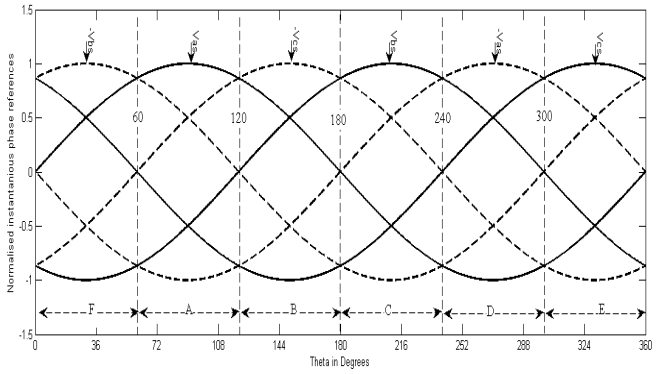

Figure. 6. Recognition of the nearest sub hexagonal centers with instantaneous reference quantities.

VI. PROPOSED DTC OF OPEN END WINDING INDUCTION MOTOR DRIVE.

The reference stator flux can either be derived from the reference speed or it can be controlled independently, while the position of the reference flux space vector can be derived from the torque error and actual rotor speed. Torque error is proportional to slip speed as explained in [2] and adding it with actual rotor speed gives the synchronous speed of the reference flux space vector. The actual stator flux space vector is derived from the motor model itself. The error between these two stator flux vectors generates the fictitious imaginary time reference vector. The d-q components of imaginary time vector can be determined from the following

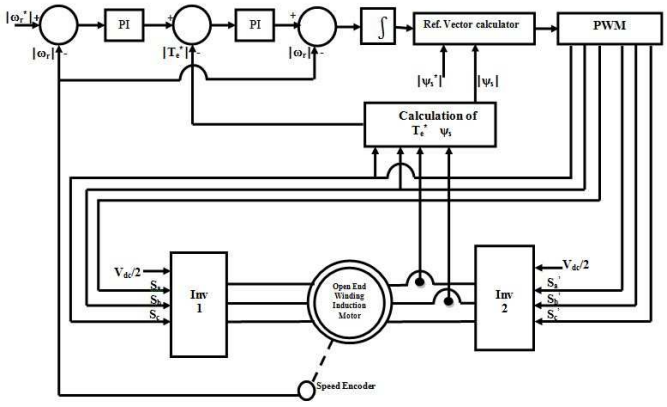

Figure 7. Control Scheme of DTC of OEWIM drive

The induction motor stator voltage equation,

$$\overline{V_s} = \frac{d\overline{\psi_s}}{dt} - \overline{I_s} R_s \qquad (6)$$

can be approximated as

$$\Delta\overline{\psi_s} = \overline{V_s} \cdot \Delta t \tag{7}$$

Over a short time period if the stator resistance is ignore from the above equations if a voltage vector is applied that changes the stator flux to increase the phase angle between the stator flux and rotor flux vectors, then the torque produced will increase. The schematic of the proposed method is as shown in Figure. 7. In this method, speed of the reference stator flux vector $|\psi^*_s|$ is derived by the addition of slip speed and actual rotor speed. The actual synchronous speed of the stator flux vector $|\psi_s|$ is calculated from the adaptive motor model. After each sampling interval, actual stator flux vector $|\psi_s|$ is corrected by the error and it tries to attain the reference flux space vector $|\psi^*_s|$. Thus the flux error is minimized in each sampling interval. In this paper, the direct axis and quadrature axis components of the reference voltage vector are created by corresponding direct axis and quadrature axes stator flux error components respectively. They derived as follows Reference value of the direct axis and quadrature axis stator fluxes and actual value of the direct axis and quadrature axis stator fluxes are compared in the reference voltage vector calculator block and hence the error in the direct and quadrature axes stator flux vectors is obtained as

$$\Delta\psi_{ds} = \psi_{ds}^{*} - \psi_{ds} \tag{8.1}$$

$$\Delta\psi_{qs} = \psi_{qs}^{*} - \psi_{qs} \tag{8.2}$$

The knowledge of flux error and stator resistive drop allows the determination of appropriate reference voltage space vectors along direct axis and quadrature axis, which is given as

$$V_{ds}^{*} = R_s I_{ds} + \frac{\Delta\psi_{ds}}{T_s} \tag{9.1}$$

$$V_{qs}^{*} = R_s I_{qs} + \frac{\Delta\psi_{qs}}{T_s} \tag{9.2}$$

The above derived direct & quadrature components of the reference voltage vector are then fed to the PWM block, from where the gating pulses for two inverters are generated.

VII. Simulation Results And Discussions

To validate the proposed method, simulation studies have been carried out by using MATLAB/SIMULINK. A 4 KW, 400V, 30 N-m, 1470 rpm, 4-pole, 50 Hz, 3-phase induction motor having the following parameters: Stator resistance Rs = 1.57ohm, rotor resistance Rr = 1.21ohm, stator inductance Ls=0.17H, rotor inductance Lr=0.17H, mutual inductance Lm=0.165H, moment of inertia J=0.089Kg-m^2. The simulation results of the proposed drive are shown in Figure 8 – Figure 25. For the decoupled method, in Figure 10, results have been shown for the starting of the motor with a reference speed command of 1200 rpm and in Figure 11 at loaded condition at t=0.6 sec here we can observe the reduction in the speed and increase in torque of the motor and reversal of the speed command of -1200 is applied at t=0.8 sec can be seen in Figure 12. Similarly Figure 15, results have been shown for the starting of the motor with a reference speed command of

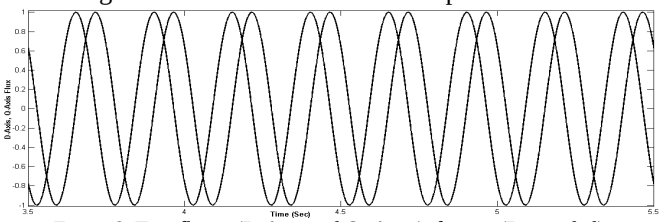

Figure 8. Two fluxes (D-Axis and Q- Axis)of stator (Decoupled)

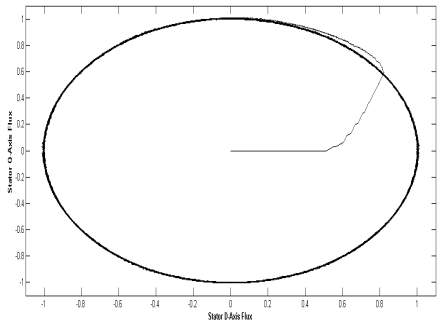

Figure 9. Stator D-Axis and Q-Axis Flux Plot (Decoupled)

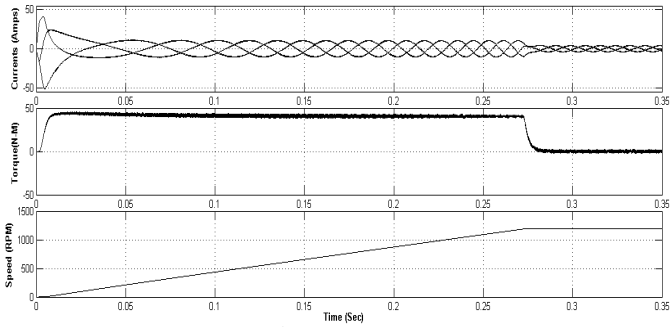

Figure 10. Change in Speed from 0 rpm to 1200pm at no-load condition (Decoupled)

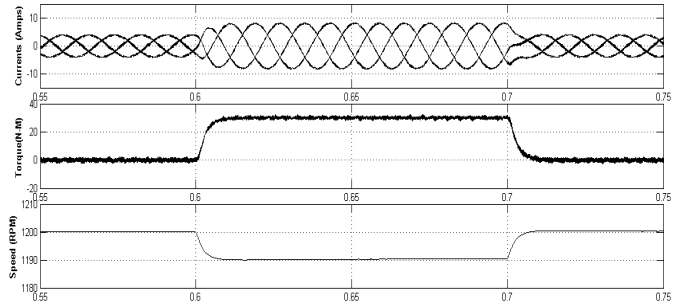

Figure 11. Change in Speed and Torque on-load condition (Decoupled)

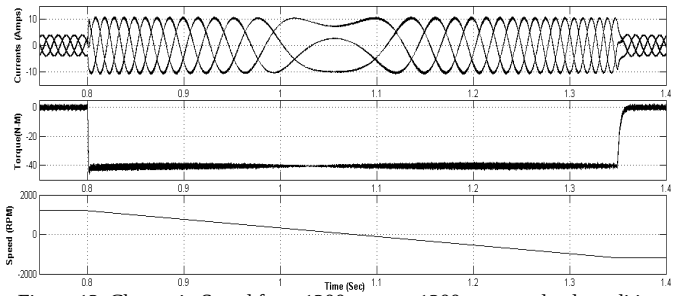

Figure 12. Change in Speed from 1200 rpm to -1200pm at no-load condition (Decoupled)

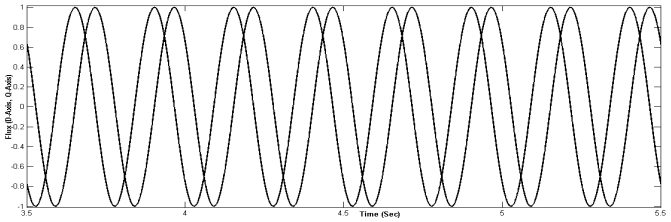

Figure 13. Two fluxes (D-Axis and Q- Axis)of stator (NSHC)

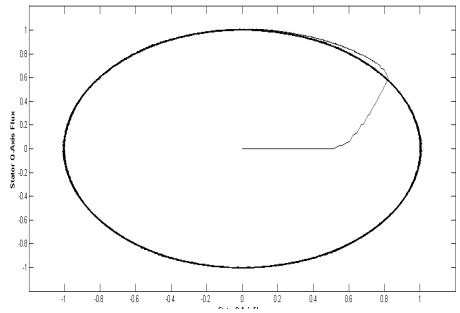

Figure 14. Stator D-Axis and Q-Axis Flux Plot (NSHC)

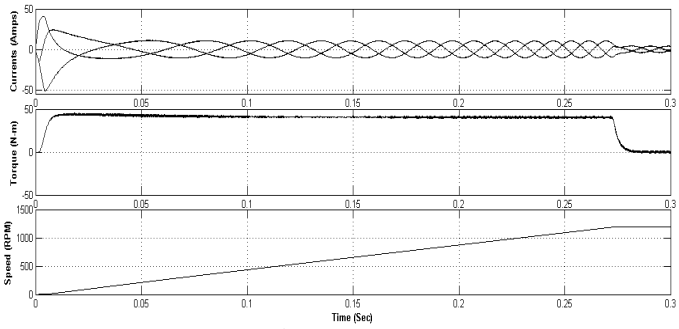

Figure 15. Change in Speed from 0 rpm to 1200pm at no-load condition (NSHC)

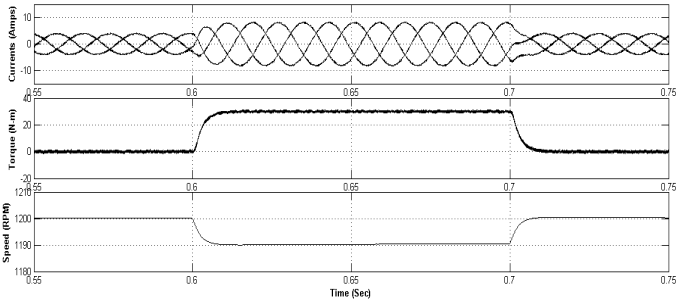

Figure 16. Change in Speed and Torque on-load condition (NSHC)

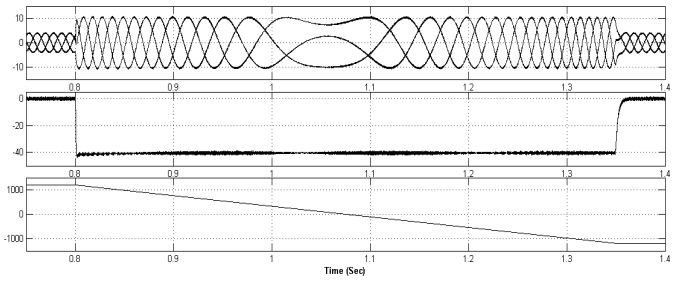

Figure 17. Change in Speed from 1200 rpm to -1200pm at no-load condition (NSHC)

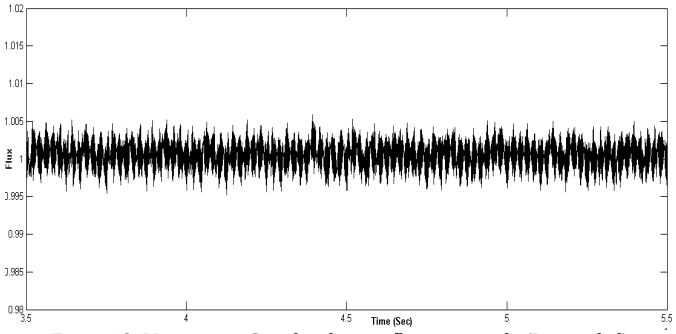

Figure 18. Variation in Simulated stator flux magnitude (Decoupled)

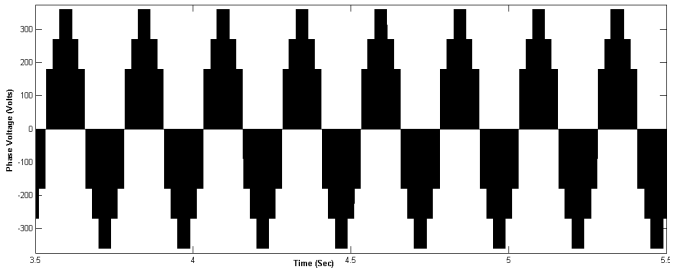

Figure 19. Effective phase voltage. (Decoupled)

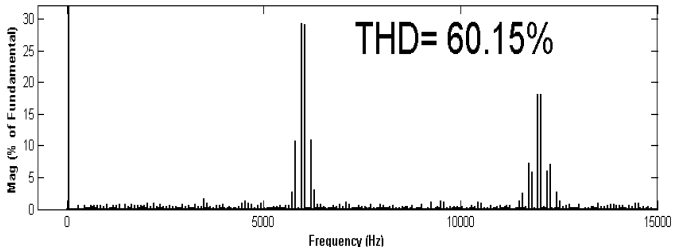

Figure 20. Voltage harmonic spectrum (Decoupled)

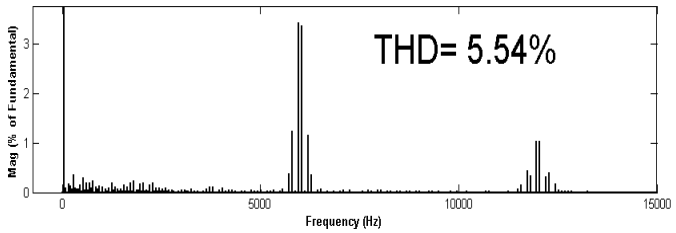

Figure 21. Current harmonic spectrum (Decoupled)

1200 rpm and in Figure 16 at loaded condition at t=0.6 sec here we can observe the reduction in the speed and increase in torque of the motor and reversal of the speed command of -1200 is applied at t=0.8 sec can be seen in Figure 17. The phase A voltage is shown in Figure 19 and 23 for Decoupled algorithm and NSHC algorithm respectively. It shows that three-level voltages are generated by two 2-level inverters for the two schemes.

Figure 20 and 24. Shows the harmonic spectra for the effective phase voltages, similarly and harmonic spectra for the phase currents can be observe d in the Figure 21 and 25 respectively. From these results it is clear that NSHC scheme is having less harmonics when compare with the decoupled strategy. The main advantage of the decoupled strategy is its fastness and simplicity so this scheme can easily implement. In the proposed methods complex calculations of regions for space

voltage vector, angle calculations sector identification are not required.

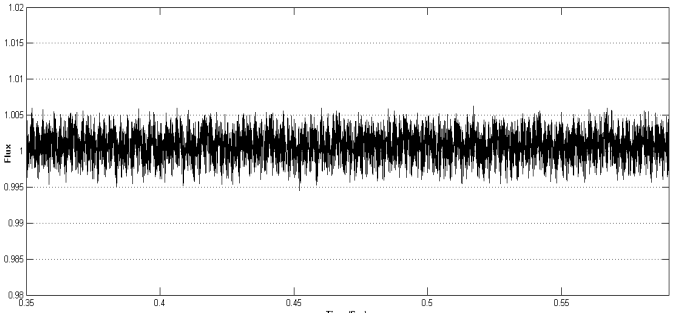

Figure 22. Variation in Simulated stator flux magnitude (NSHC)

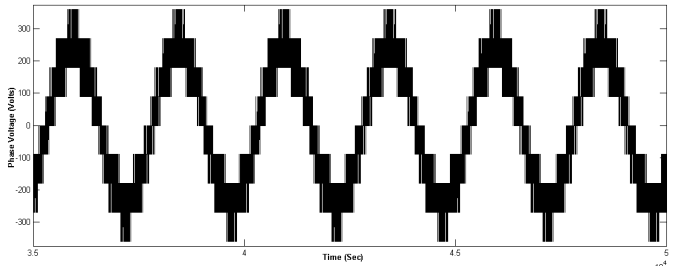

Figure 23. Effective phase voltage. (NSHC)

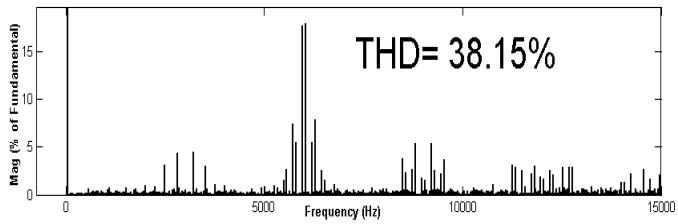

Figure 24. Voltage harmonic spectrum (NSHC)

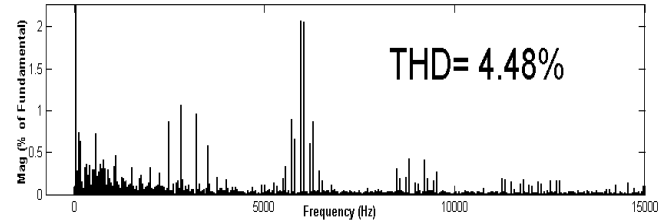

Figure 25. Current harmonic spectrum (NSHC)

VIII. CONCLUSION

The described PWM schemes use only the three instantaneous phase reference voltages for the implementation. the control strategies proposed for reducing the switching frequency the inverters, with lesser complexity compared to the multi-level inverter, also suitable for the high power applications. Also the proposed control strategies are very simple as they do not require dividing the operating region into sub-sectors/sectors. Determining the sectors and angle of voltage vector is eliminated. Due to the three level voltage generation, torque and current waveforms are superior to that of basic direct torque control scheme. The methods proposed for the DTC of the Open End Winding Induction Motor gives a result in the reduction of the ripple and harmonics and distortion of stator current. In these two approaches the decoupled method is having same frequency of the operation and the two inverters are switched in the switching time period and in the alternate inverter switching one inverter is completely clamped and other is switched therefore the two inverters share the load equally and the switching time is reduced half of the switching time required in decoupled algorithm. The current wave forms are superior in case of the alternative inverter switching than the decoupled switching. The performance of the proposed control strategy improves towards full load as both the inverters are operated and equally loaded.

REFERENCES

[1] EG Shivakumar, K Gopakumar, SK Sinha, VT Rangnathan, "Space Vector PWM Control of Dual Inverter Fed Open-End Winding Induction Motor Drive," IEEE-APEC, Vol.1, 2001, pp 399-405.

[2] I Takahashi and T Noguchi, "A New Quick- Response and High-Efficiency Control of an Induction Motor," IEEE Trans. Industry Applications, Vol. IA-22, No.5, 1986, pp 820-827.

[3] I Takahashi and Youchi Ohmori, "High- Performance Direct Torque Control of an Induction Motor," IEEE Trans. Industry Applications, Vol. IA-25, No.2, 1989, pp 257-264.

[4] Janssen, M. Steimel, A. "Direct Self Control With Minimum Torque Ripple and High Dynamics for Double three-level GTO Inverter Drive," IEEE Trans. On Industrial Electronics, Vol.49, No.5, 2002, pp 1065-1071.

[5] Brain A Welchko and James M Nagashima, "A Comparative Evaluation of Motor Drive Topologies for Low-Voltage, High-Power EV/HEV Propulsion Systems," IEEE International Symposium on Industrial Electronics, ISIE'03, Brazil, 2003, pp 1-6.

[6] Arbind Kumar, BG Fernandes, K Chatterjee, "DTC of Open-End Winding Induction Motor Drive Using Space Vector Modulation With Reduced Switching Frequency," IEEE-PESC, 2004, pp 1214-1219.

[7] G.Satheesh, T. Bramhananda Reddy and Ch. Sai Babu, "Novel SVPWM Algorithm for Open end Winding Induction Motor Drive Using the Concept of Imaginary switching Times" IJAST, Vol. 2, No.4, 2011, pp 44- 92.

[8] Nabae, A., Takahashi, I., and Akagi, H.: 'A neutral-point clamped PWM inverter', IEEE- Trans. Ind. Appl., 1981, 17, (5), pp. 518–523

[9] S.Srinivas and V.T.Somasekhar, "Space Vector Based PWM switching strategies for a 3 level dual inverter fed open end winding induction m otor drive and their comparative evaluation" IET-Electr. Power Appl., Vol 2, No.1, January 2008, PP19-31.

[10] Joohn-Sheok Kim and Seung-Ki Sul, "A novel voltage modulation technique of the space vector PWM", in Conf. Rec. IPEC'95, Yokohama, Japan, 1995, pp. 742-747.

Authors Profile

Satheesh G received the B.E degree from Bangalore University in 2001, the M.Tech degree from JNT University, Anantapur, India in the year 2004, and is currently pursuing the Ph.D. in Electrical Engineering Department, JNTU, Kakinada.

His areas of interest include Power Electronics, pulse width modulation techniques, AC Drives and Control.

Dr. T. Bramhananda Reddy was born in 1979. He graduated from Sri Krishna Devaraya University, Anantapur in the year 2001. He received M.E degree from Osmania University, Hyderabad, India in the year 2003. He is presently Associate Professor in the Electrical and Electronics Engineering Department, G. Pulla Reddy Engineering College, Kurnool, India. He presented more than 35 research papers in various national and international conferences and journals.

His research areas include PWM techniques, DC to AC converters and induction motor drives.

Dr. Ch. Sai Babu received the B.E from Andhra University (Electrical & Electronics Engineering), M.Tech in Electrical Machines and Industrial Drives from REC, Warangal and Ph.D in Reliability Studies of HVDC Converters from JNTU, Hyderabad. Currently he is working as a Professor in Dept. of EEE in JNTUCEK, Kakinada. He has published several National and International Journals and Conferences.

His area of interest is Power Electronics and Drives, Power System Reliability, HVDC Converter Reliability, Optimization of Electrical Systems and Real Time Energy Management.